


**Universal semiclassical equations based on the quantum metric for a two-band system**C. Leblanc<sup>1</sup>, G. Malpuech<sup>1</sup> and D. D. Solnyshkov<sup>1,2</sup><sup>1</sup>*Institut Pascal, PHOTON-N2, Université Clermont Auvergne, CNRS, SIGMA Clermont, F-63000 Clermont-Ferrand, France*<sup>2</sup>*Institut Universitaire de France (IUF), F-75231 Paris, France* (Received 23 June 2021; revised 7 September 2021; accepted 8 October 2021; published 26 October 2021)

We derive semiclassical equations of motion for an accelerated wave packet in a two-band system. We show that these equations can be formulated in terms of the static band geometry described by the quantum metric. We consider the specific cases of the Rashba Hamiltonian with and without a Zeeman term. The semiclassical trajectories are in full agreement with the ones found by solving the Schrödinger equation. This formalism successfully describes the adiabatic limit and the anomalous Hall effect traditionally attributed to Berry curvature. It also describes the opposite limit of coherent band superposition, giving rise to a spatially oscillating Zitterbewegung motion, and all intermediate cases. At  $k = 0$ , such a wave packet exhibits a circular trajectory in real space, with its radius given by the square root of the quantum metric. This quantity appears as a universal length scale, providing a geometrical origin of the Compton wavelength. The quantum metric semiclassical approach could be extended to an arbitrary number of bands.

DOI: [10.1103/PhysRevB.104.134312](https://doi.org/10.1103/PhysRevB.104.134312)**I. INTRODUCTION**

General relativity is the first example of a geometrical theory of motion, where the particle trajectories are not governed by gravitational forces, but are found as the geodesics of the space-time metric. In a completely different perspective, the semiclassical theory of electron dynamics in solids was derived in the 1930s from quantum mechanics [1,2], involving as a key element the wave-vector-dependent group velocity. These equations have been corrected in 1999 [3] to include the impact of the Berry curvature and describe the anomalous Hall effect (AHE). The AHE was discovered in the 1950s [4], but the deep understanding of the underlying physics and of its importance came with its description in terms of geometrical properties of the quantum space.

Indeed, the geometry of the quantum space has been actively studied since the 1980s [5–7], bringing the description of the quantum Hall effect [8,9], and the forthcoming enormous development of topological physics [10–13]. The geometrical information about the eigenstates of a Hamiltonian is contained in the gauge-invariant quantum geometric tensor, whose symmetric real part defines the quantum metric (QM) characterizing distances between states [5] in a parameter space. Its antisymmetric imaginary part determines the Berry curvature [6]. The key hypothesis of the Niu-Sundaram [3,14] equations is the adiabatic approximation, when the wave packet remains in a single energy band, as in the original work of Berry [6]. The extension to the situation where several bands have comparable populations was done in Ref. [15], but using time-dependent components of the generalized Berry curvature tensor, which depend on initial conditions and not only on static band parameters. Multiband Bloch oscillations with non-Abelian Berry curvature were recently studied in Ref. [16].

The potential roles of the QM have been more recently underlined in the calculations in quantum informatics, quan-

tum phase transitions [17], magnetic susceptibility [18,19], excitonic levels [20], and superfluidity in flat bands [21,22]. The QM is now explicitly accounted for in the design and engineering of topological systems [23,24], and its integral is linked with the Chern number [19,25–28]. Experimental measurements of the QM in different systems also start to appear [29–31]. In particular, it is well understood that the QM should appear in the description of transitions between quantum levels. For example, it allows one to describe small nonadiabatic corrections to the AHE [18,32,33]. In some cases, the QM was even found to dominate the dynamics. This occurs in systems with nonreciprocal directional dichroism [34] and also in strongly non-Hermitian systems in the vicinity of the exceptional points, where the evolution can never be adiabatic [35]. A situation of a particular interest occurs in spin-orbit-coupled systems [36–39] which can be described in terms of non-Abelian gauge potentials [40,41] with emergent vectorial charges [42,43]. The resulting Zitterbewegung (ZBW) motion [44,45] involves a coherent superposition of several bands. The ZBW is studied theoretically and experimentally in various electronic [46–48], atomic [49–51], and photonic systems [52–55] including polaritons [56,57]. This is an appealing situation for its description in terms of QM, as noticed in Ref. [58], where the QM was shown to be responsible for a contribution to the effective mass.

In this work, we derive semiclassical equations of motion in a two-band system using only the static band geometry encoded in the QM. The solutions of these new equations are in complete agreement with the direct numerical solutions of the Schrödinger equations for all the cases we considered. They describe the AHE, traditionally attributed to Berry curvature. They also describe the opposite limit, when the wave packet is coherently distributed over the two bands, and in particular the ZBW motion induced by an emergent non-Abelian gauge field. We show that a wave packet centered at  $k = 0$  exhibits a circular trajectory in real space, with its radius given by the

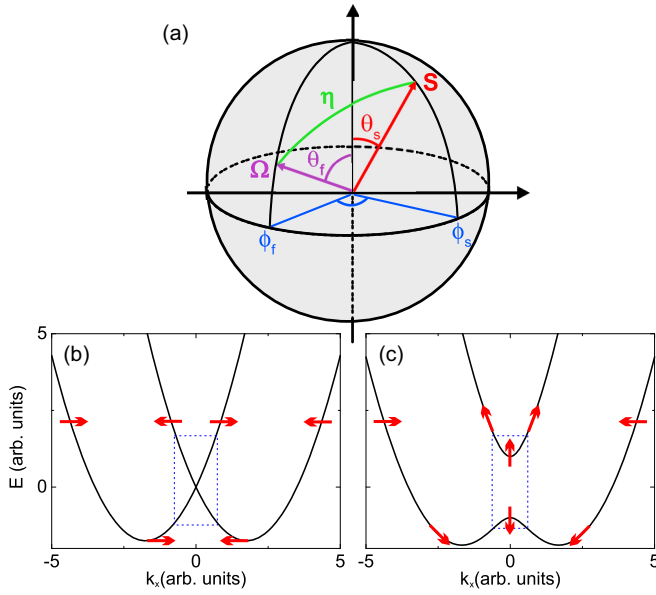


FIG. 1. (a) Bloch sphere representation showing the pseudospin  $\mathbf{S}$ , the effective field  $\mathbf{\Omega}$ , and their polar and azimuthal angles  $\theta$  and  $\phi$ . The angle between the spin and the field is  $\eta$ . (b), (c) Dispersion along  $k_x$  of the eigenmodes of the (b) Rashba and (c) Rashba+Zeeman Hamiltonians. The red arrows show the pseudospin orientation of the modes.

square root of the quantum metric. This quantity appears as a universal length scale, determining the uncertainty of the position of a particle involving several bands. It provides a geometrical origin of the Compton wavelength.

## II. THE MODEL

We begin with the Hamilton's equations of motion for a wave packet. Working with a two-band system allows us to use the mapping to the pseudospin  $\mathbf{S}$  interacting with an effective magnetic field  $\mathbf{\Omega}$  [59], with the Hamiltonian given by  $H = -\hbar\mathbf{\Omega} \cdot \mathbf{S}/2$ , and the associated geometry of the Bloch sphere (Fig. 1). A general superposition of two eigenstates can be written as

$$|\psi\rangle = c_1|\psi_1\rangle + c_2|\psi_2\rangle, \quad (1)$$

with  $c_1 = \cos\theta_s/2e^{-i\phi_s}$  and  $c_2 = \sin\theta_s/2$ , where  $\theta_s$  and  $\phi_s$  are the time-dependent angles, giving the orientation of the pseudospin on the Bloch sphere. The equations of motion for the spatial degrees of freedom are therefore accompanied

with the precession equation for the pseudospin describing the wave packet distribution within the two bands:

$$\dot{\mathbf{p}} = -\frac{\partial H}{\partial \mathbf{r}}, \quad \dot{\mathbf{r}} = \frac{\partial H}{\partial \mathbf{p}}, \quad \dot{\mathbf{S}} = \mathbf{S} \times \mathbf{\Omega}. \quad (2)$$

Here,  $\mathbf{r}$  is the spatial coordinate of the wave packet center of mass,  $\mathbf{p} = \hbar\mathbf{k}$  is the center-of-mass momentum of the wave packet ( $\mathbf{k}$  is the center-of-mass wave vector). The wave packet is considered as a classical pointlike particle and its distribution over the bands is encoded in its pseudospin vector. At a given moment of time, the effective field is  $\mathbf{\Omega}(\mathbf{k}(t))$  and the pseudospin is  $\mathbf{S}(t)$ , shown in Fig. 1 with violet and red arrows, respectively. While it is often possible to convert Hamilton's equations to geodesics equation in an abstract metric [60], our goal is rather to elucidate the role of the QM, while keeping the other coordinates intact.

The first of Eqs. (2) describes the acceleration of the wave packet due to a spatial gradient of the potential. We will rather focus on the second of Eqs. (2), describing the group velocity. The Hamilton's function  $H$  corresponds to the energy  $E = \langle \psi | \hat{H} | \psi \rangle$  of the full wave packet. It depends on the wave vector both directly, via the band dispersion  $E_i(\mathbf{k})$ , and indirectly, via the fractions  $f_i = |c_i|^2$ . This energy can be rewritten as  $E = f_1E_1 + f_2E_2 = (f_1 + f_2)\bar{E} + (f_2 - f_1)\hbar\Omega$  where  $\bar{E}$  is the spinless part of the dispersion and  $\Omega$  is the absolute value of the effective field.

We characterize the pseudospin  $\mathbf{S}$  and the effective field  $\mathbf{\Omega}$  by the respective spherical coordinates  $\theta_s, \phi_s$  and  $\theta_f, \phi_f$  (see Fig. 1). The fractions  $f_i$  are determined by the distance between these two vectors on the Bloch sphere  $\eta$  as  $f_{1,2} = (1 \pm \cos\eta)/2$ , and this distance can be found from the spherical law of cosines (see Appendix A). Our key idea is to use the QM as the link between the angles on the Bloch sphere and the wave vectors. By definition, the QM provides a link between the quantum distance  $ds$  and the distance in reciprocal space:

$$ds^2 = g_{k_i, k_j} dk_i dk_j, \quad (3)$$

with the QM defined by

$$g_{ij} = \text{Re} \left[ \left\langle \frac{\partial \psi_1}{\partial k_i} \left| \frac{\partial \psi_1}{\partial k_j} \right\rangle - \left\langle \psi_1 \left| \frac{\partial \psi_1}{\partial k_i} \right\rangle \left\langle \frac{\partial \psi_1}{\partial k_j} \left| \psi_1 \right\rangle \right]. \quad (4)$$

The corresponding quantum distance for the displacement  $d\eta$  on the Bloch sphere is  $ds^2 = (d\eta)^2/4$ . Ultimately, the equations of motion read (see Appendix A for details):

$$\hbar\dot{\mathbf{k}} = -\frac{\partial E}{\partial \mathbf{r}}, \quad \dot{\mathbf{S}} = \mathbf{S} \times \mathbf{\Omega}, \quad (5)$$

$$\begin{aligned} \hbar\dot{\mathbf{r}} = & \frac{\partial \bar{E}}{\partial \mathbf{k}} - 2\frac{\partial \hbar\Omega}{\partial \mathbf{k}}(\cos\theta_s \cos\theta_f + \sin\theta_s \sin\theta_f \cos(\phi_f - \phi_s)) \\ & - \hbar\Omega\sqrt{g_{\mathbf{k}\mathbf{k}}} \frac{[(-\cos\theta_s \sin\theta_f + \sin\theta_s \cos\theta_f \cos(\phi_f - \phi_s)) - \sin\theta_s \sin(\phi_f - \phi_s) \sin\theta_f \left(\frac{\partial \phi_f}{\partial \theta_f}\right)]}{\sqrt{1 + \sin^2\theta_f \left(\frac{\partial \phi_f}{\partial \theta_f}\right)^2}}. \end{aligned} \quad (6)$$

In these expressions, the QM  $\sqrt{g_{\mathbf{k}\mathbf{k}}} = (\sqrt{g_{k_x, k_x}}, \sqrt{g_{k_y, k_y}})^T$  is that of a single band (the lowest energy band of the doublet). We see that the QM appears as an overall factor of the corresponding term, entering (6) together with  $\Omega$  and thus completely determining

the scale of the corresponding physical effect. The physical meaning of this term is the modification of the energy of the wave packet due to its redistribution over the two bands with the rotation of the spin, and this is controlled by the QM.

A similar system of equations can be derived from the Hamilton's equations for an arbitrary number of bands. As in the two-band case, the terms containing the QM appear from the variation of the fractions  $\partial f_i / \partial k_j$ : the variation of the overlap integral is determined by the variation of the length of the corresponding geodesic curve, which is entirely determined by the product of the quantum metric  $g_{k,k}$  and the projection of the displacement  $\delta k_j$  on the geodesic's tangent vector, according to the well-known theorem from the differential geometry [61]. We leave this for future work.

Although this equation does not include the Berry curvature explicitly, it allows us to recover the semiclassical equations of Ref. [3] with the Berry curvature terms in the adiabatic limit (see Appendix B). In spite of being written only in terms of the QM, it entirely describes the AHE drift, and allows us to go far beyond it, as we show below. In other words, being derived from the Hamilton's equations (2) without any additional approximations, Eqs. (5) and (6) are valid up to arbitrary order in the field strength, being limited only by the requirement of wave packet localization [62]. Another advantage of Eqs. (5) and (6) is that they contain only the static properties of the bands. These equations could also be extended to account for a magnetic field by including it into the equations for the momentum and for the pseudospin dynamics (5) [18,63].

If the Hamiltonian is such that the effective field remains for all  $k$  in the equatorial plane ( $\theta_f = \pi/2$ ,  $\partial \phi_f / \partial \theta_f = \infty$ ), as is the case for the massless Dirac, Rashba, Dresselhaus, and transverse electric-transverse magnetic (TE-TM) [64] Hamiltonians, Eq. (6) is considerably simplified, reducing to

$$\hbar \dot{\mathbf{r}} = \frac{\partial E}{\partial \mathbf{k}} + \hbar \Omega \sqrt{g_{kk}} \sin \theta_s \sin(\phi_f - \phi_s) \quad (7)$$

with  $E = \bar{E} + \hbar \Omega (\cos \theta_s \cos \theta_f + \sin \theta_s \sin \theta_f \cos(\phi_f - \phi_s))$ . In what follows, we consider a Rashba Hamiltonian extensively studied in electronics, spintronics, and photonics, both with and without a Zeeman field:

$$\hat{H} = \frac{\hbar^2 k^2}{2m} + \alpha \mathbf{k} \cdot \boldsymbol{\sigma} + \Delta \sigma_z, \quad (8)$$

where  $\boldsymbol{\sigma}$  is a vector of Pauli matrices,  $\alpha$  is the Rashba magnitude, and  $\Delta$  the magnitude of the effective Zeeman field. When  $\Delta = 0$ , the eigenvalues are  $E_{\pm} = \hbar^2 k^2 / (2m) \pm \alpha k$ , plotted in Fig. 1(b). Close to  $k = 0$ , the Hamiltonian is analogous to a two-dimensional (2D) massless Dirac Hamiltonian, with  $\alpha$  playing the role of the speed of light  $c$ . The bands have no distributed Berry curvature. A nonzero Zeeman field opens a gap at  $k = 0$  [Fig. 1(c)], making appear an effective mass  $m_{eff} = \hbar^2 \Delta^2 / \alpha^2$  (equivalence with a massive Dirac Hamiltonian). The corresponding bands show a nonzero distributed Berry curvature (see Appendix B). We are now going to consider the wave packet motion in these two situations.

### III. RESULTS AND DISCUSSION

#### A. Crossing bands: Rashba SOC (Dirac cone)

The equation of motion (7) writes explicitly

$$\dot{\mathbf{r}} = \left( \frac{\hbar k}{m} + \frac{\alpha}{\hbar} \cos(\phi_s - \phi_k) \sin \theta_s \right) \begin{pmatrix} \cos \phi_k \\ \sin \phi_k \end{pmatrix} + \Omega \sin \theta_s \sin(\phi_k - \phi_s) \begin{pmatrix} \sqrt{g_{k_x k_x}} \\ \sqrt{g_{k_y k_y}} \end{pmatrix}, \quad (9)$$

where  $\phi_k$  is the polar angle of the wave vector, to which the effective field is antiparallel ( $\phi_f = \phi_k - \pi$ ). This equation contains only the orientation of the spinor  $\theta_s$ ,  $\phi_s$  and the center-of-mass wave vector  $k$ . The first part of the group velocity contains the spin-independent parabolic dispersion and a spin-dependent contribution, with the propagation direction ultimately controlled by the current orientation of the spinor. The second part of this expression, which includes the QM  $g_{kk}$ , appears because of the explicit time dependence of the spinor. The  $x$  and  $y$  projections of the velocity are controlled by the corresponding projections of the QM.

As an illustration, we consider the case without external fields ( $\dot{k} = 0$ ), with  $\mathbf{k} = k_0 \mathbf{e}_x$  ( $\phi_k = 0$ ), and the spinor  $\mathbf{S} = S_z \mathbf{e}_z$  perpendicular to the effective field at  $t = 0$ , so  $\theta_s = 0$ . The wave function is projected equally on both bands, and the pseudospin precession frequency is  $\Omega = 2\alpha k_0 / \hbar$ .

In this case, the  $x$  projection of the group velocity is constant. The time-dependent trajectory reads

$$x(t) = \frac{\hbar k_0}{m} t$$

$$y(t) = (1 - \cos \Omega t) \sqrt{g_{k_y k_y}} = \frac{1 - \cos \Omega t}{2k_0} \quad (10)$$

because the QM is  $g_{k_y k_y} = 1/4k_0^2$ . This oscillating motion due to the pseudospin precession is the ZBW effect. The magnitude of the oscillation along  $y$  is given by  $\sqrt{g_{k_y k_y}}$ , which acts as a fundamental characteristic length scale of the problem, as we will discuss more in details below.

To confirm our analytical results, we perform numerical simulations, solving the time-dependent 2D spinor Schrödinger equation

$$i\hbar \frac{\partial \psi}{\partial t} = \hat{H} \psi \quad (11)$$

with the Rashba Hamiltonian (8), taking a finite-size Gaussian wave packet  $\psi_0 = \exp(-(\mathbf{r} - \mathbf{r}_0)^2 / 2\sigma^2) \exp(i\mathbf{k}_0 \mathbf{r})$  of a width  $\sigma$  in real space (and  $1/\sigma$  in reciprocal space) centered at a wave vector  $k_0$ , with its spinor part given by  $(1, 0)^T$  (corresponding to  $\theta_s = 0$ ) as an initial condition. We choose the simulation parameters typical for polaritonic systems [31]:  $\alpha = 1 \text{ meV}/\mu\text{m}^{-1}$ ,  $k_0 = 1 \mu\text{m}^{-1}$ ,  $m = 2 \times 10^{-5} m_0$  ( $m_0$  is the free electron mass),  $\sigma = 128 \mu\text{m}$ . We can observe a truly excellent agreement with the analytical trajectory (Fig. 2) in a substantial time window, limited only by the transient nature of the ZBW due to the finite wave packet size in numerical simulations [62].

As said in the introduction, the Rashba Hamiltonian can be described as resulting from the action of a non-Abelian gauge field [36–39] described by the Yang-Mills Lagrangian [40].

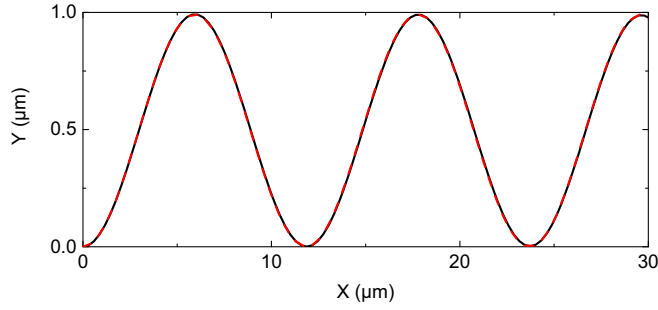


FIG. 2. Rashba Hamiltonian. Wave packet dynamics from Schrödinger equation (black solid line) and analytical solution of semiclassical Eqs. (5) and (6) (red dashed line).

Within this picture, it is also possible to derive a semiclassical equation of motion, where the acceleration is the result of the action of a non-Abelian magnetic force acting on (pseudo)-spin currents, as recently measured in Ref. [45]. As shown in the Appendix D section, the time derivative of Eq. (9) gives an expression of the transverse acceleration in terms of the QM, equivalent to the results of the Yang-Mills theory [37]. This acceleration appears because of the precession of the spin, or, in other words, because of the interband transitions described by the QM. This provides a microscopic mechanism behind the non-Abelian Lorentz force of the Yang-Mills field, which can be interpreted as being the consequence of the geometry of the underlying quantum space.

### B. Anticrossing bands: Rashba+Zeeman (massive Dirac)

We now consider the Rashba Hamiltonian combined with a Zeeman term. The resulting bands are non-degenerate and show a distributed Berry curvature. A wave packet accelerated in such a system can show either AHE or ZBW, or a combination of both effects, depending on initial conditions. Figures 3(a)–3(c) considers the acceleration by a spatial energy gradient  $2 \times 10^{-3}$  meV/ $\mu\text{m}$  for different initial conditions. We compare the center-of-mass trajectories obtained by solving the spinor Schrödinger equation (11) and the ones obtained from the semiclassical equations of motion (6). The Zeeman splitting is  $\Delta = 0.5$  meV, other parameters as above. Panel (a) demonstrates the AHE regime, with the initial condition corresponding to an eigenstate of the system (the lowest energy band at  $k = 0$ ): the deviation along  $y$  is the AHE drift. The correspondence between the description of the AHE in terms of Berry curvature and the one based on the use of the QM is explicitly shown in the Appendix B section. Panel (b) corresponds to the pure ZBW, with the initial condition corresponding to the equal fraction of both branches:  $f_1 = f_2$ . In this case, there is no AHE drift, because the effect of the Berry curvature is completely canceled by  $f_1 - f_2 = 0$ . Finally, panel (c) corresponds to a particular case of  $f_1 - f_2 = 0.9$ , allowing us to observe both the AHE drift and the large oscillations due to the ZBW. Qualitatively similar results are obtained with a TE-TM spin-orbit coupling (SOC) (see Appendix E) characterized by a double winding number and typical for photonic systems. The AHE has been recently measured in an optical system with TE-TM SOC and Zeeman splitting [31].

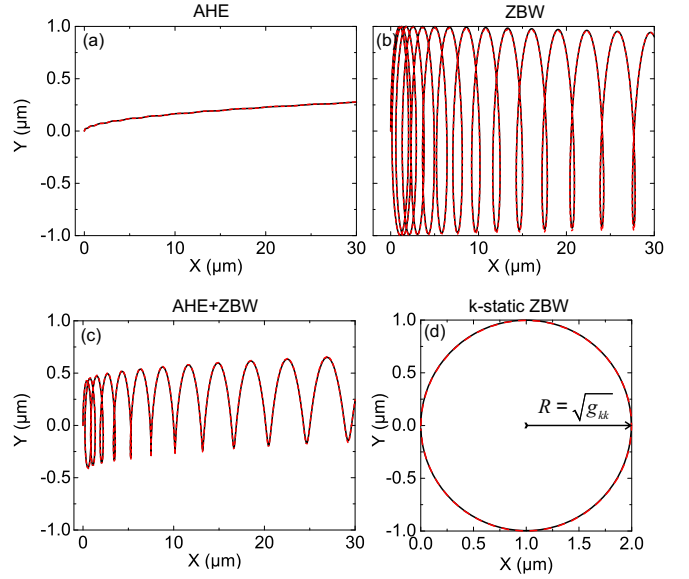


FIG. 3. Rashba+Zeeman Hamiltonian. Wave packet dynamics from Schrödinger (black solid lines) and semiclassical (red dashed lines) equations: (a) AHE (single-band initial excitation); (b) ZBW (equal fractions of both bands); (c) both effects together; (d) cyclotronlike orbits at constant  $k$  (no potential gradient) with a radius determined by the metric.

If we consider a wave packet with zero initial wave vector and zero external force  $\dot{k} = 0$ , the effective field is completely determined by the Zeeman splitting:  $\theta_f = 0$ . If the spin of the initial wave packet is in the plane  $\theta_s = \pi/2$  (and  $\phi_s = 0$  as an example), the third equation of motion (5) gives that the spin will remain in the plane ( $\sin \theta_s = 1$ ) and rotate with an angular frequency  $\Omega$  ( $\phi_s = \Omega t$ ). Equation (6) gives

$$\dot{x} = \Omega \sqrt{g_{k_x k_x}} \cos \Omega t, \quad \dot{y} = \Omega \sqrt{g_{k_y k_y}} \sin \Omega t, \quad (12)$$

where the QM at  $k = 0$  is given by  $g_{k_x k_x} = g_{k_y k_y} = \alpha^2 / 4\Delta^2$ . These equations explicitly show the wave packet rotation in real space, with a radius determined by the value of the QM  $R = \sqrt{g_{kk}} = \alpha / 2\Delta$ , as illustrated in Fig. 3(d).

Our results show that the QM provides a characteristic length scale  $l = \sqrt{g_{\max}}$  for the semiclassical behavior. This is best seen with the example of the Dirac equation, where the value of the QM at  $k = 0$  is

$$\sqrt{g_{kk}} = \frac{\hbar}{mc}, \quad (13)$$

which is the well-known Compton wavelength  $\lambda_C$  of the electron, determining a universal length scale in Physics. Indeed, it enters the expressions for the classical electron radius, the Bohr radius, the electron-proton scattering cross section, and even determines the Planck length. We note that the full Dirac equation contains four components, and the QM associated with both the particle-antiparticle and the spin degrees of freedom is the same, determined by the relativistic effects.

The physical meaning of the Compton wavelength can be understood with the QM. Qualitatively, it limits the precision of the measurement of the electron's position. Indeed, scattering of a photon with the wavelength  $\lambda_C$  brings the electron into a 50% electron-positron superposition, corresponding exactly



to the case of Fig. 3(d): the electron's center of mass exhibits a cyclotron motion with the radius  $R = \sqrt{g_{kk}(0)} = \lambda_C$ . This rotation is what determines the uncertainty of its position. Even for Hamiltonians which do not have a single length scale, the QM still can be used to determine the scales of the ZBW at rest or at high velocities, changing from the Compton to the de Broglie wavelength [46,47]: indeed,  $\sqrt{g_{kk}} \sim 1/k = \hbar/p$  at large  $k$ .

The maximal value of the trace of the QM is an important physical quantity. This maximal value determines the extension of the metric in the parameter space, that is, the characteristic scale at which the changes occur (for example, level crossing), because the integral of the QM (approximately, the product of the maximal value and the extension) is often quantized, representing a topological invariant [28] similar to the Chern number. It determines both the maximal amplitude of the ZBW oscillations and of the anomalous Hall drift (even though the latter is an integral quantity). It determines the spatial extension of the chiral edge state in topological insulators, controlling the minimal size of topological lasers and optical isolators. This will be a subject for future works.

#### IV. CONCLUSIONS

We derived the semiclassical equations of motion for a wave packet in a two-band system in terms of the static band parameters, in particular, the QM. The latter turns out to determine a universal length scale for all effects beyond the simple group velocity.

#### ACKNOWLEDGMENTS

We acknowledge useful discussions with V. Rabant. We acknowledge the support of the project Quantum fluids of light (ANR-16-CE30-0021), of the ANR Labex GaNEXT (ANR-11-LABX-0014), and of the ANR program "Investissements d'Avenir" through the IDEX-ISITE initiative 16-IDEX-0001 (CAP 20-25).

#### APPENDIX A: SPHERICAL ANGLES AND THE QUANTUM METRIC

The equation for the angle  $\eta$  given by the spherical cosine law reads:

$$\cos \eta = \cos \theta_s \cos \theta_f + \sin \theta_s \sin \theta_f \cos(\phi_f - \phi_s). \quad (\text{A1})$$

The contribution to the spin-dependent part of the energy stemming from the wave-vector dependence of the coefficients  $f_i$  can be found via the wave-vector dependence of the spherical coordinates  $\theta_f$ ,  $\phi_f$  of the effective field:

$$\frac{\partial f_i}{\partial k_j} = \frac{\partial f_i}{\partial \phi_f} \frac{\partial \phi_f}{\partial k_j} + \frac{\partial f_i}{\partial \theta_f} \frac{\partial \theta_f}{\partial k_j} \quad (\text{A2})$$

and the latter are determined by the metric part of the quantum geometric tensor [5]. This allows writing

$$\frac{\partial \theta_f}{\partial k_i} = 2\sqrt{g_{k_i k_i}} \cos \zeta, \quad \frac{\partial \phi_f}{\partial k_i} = 2\sqrt{g_{k_i k_i}} \frac{\sin \zeta}{\sin \theta_f} \quad (\text{A3})$$

with  $\zeta$  controlled by the evolution of the effective field with  $k_i$  as  $\tan \zeta = \sin \theta_f (\partial \phi_f / \partial \theta_f)_i$ .

We note that a nonzero Berry curvature requires the effective field to cover a solid angle on the Bloch sphere, that is, the effective field should move along different axes, which means different values of  $\zeta$  for  $k_x$  and  $k_y$ . Different terms will therefore appear in the equations for the two projections of the velocity.

#### APPENDIX B: BERRY CURVATURE AND QUANTUM METRIC

The one-to-one correspondence between the Berry curvature and the QM in two-band systems was discussed in Refs. [19,25,26], and this discussion was extended to three-band systems in Ref. [65]. Given the existence of such mapping, it is therefore natural that it is possible to write the semiclassical equations in the adiabatic limit using either the Berry curvature or the QM. Here, we demonstrate that the Berry curvature term responsible for the AHE drift gives exactly the same contribution to the transverse group velocity as the term written in the equation using the QM.

In the particular case of the Rashba SOC with the Zeeman splitting we consider that, as an example, the AHE drift occurs in the  $y$  direction. Therefore, we need to study the  $y$  projection of the group velocity. To establish the equivalence between the equations with the Berry curvature, containing the time derivative of the wave vector  $dk_y/dt$  and the semiclassical equations with the QM, we will use the description of the nonadiabaticity by the QM.

We begin by providing the explicit expressions for the Berry curvature and the quantum metric for the Rashba/Zeeman Hamiltonian, equivalent to the massive Dirac Hamiltonian. The Berry curvature reads

$$B_z = \frac{\alpha^2 \Delta}{2(\Delta^2 + \alpha^2 k^2)^{3/2}} \quad (\text{B1})$$

and the QM reads

$$g_{k_x, k_x} = \frac{\alpha^2 (\Delta^2 + \alpha^2 k_y^2)}{4(\Delta^2 + \alpha^2 k^2)^2}, \quad g_{k_y, k_y} = \frac{\alpha^2 (\Delta^2 + \alpha^2 k_x^2)}{4(\Delta^2 + \alpha^2 k^2)^2}. \quad (\text{B2})$$

The term of Eq. (6) of the main text responsible for the transverse anomalous Hall velocity (for a wave packet characterized by a wave vector along  $x$ ) reads

$$\hbar v_y = \dots + \hbar \Omega \sqrt{g_{k_y, k_y}} \sin \theta_s \sin(\phi_f - \phi_s). \quad (\text{B3})$$

In the quadiabatic regime,  $\sin \theta_s \approx \sin \theta_f = \alpha k / \hbar \Omega$  and  $\sin(\phi_f - \phi_s) \approx \eta / \sin \theta_f$ , which gives

$$\hbar v_y = \dots + \hbar \Omega \sqrt{g_{k_y, k_y}} \eta. \quad (\text{B4})$$

The angle  $\eta$  here can be obtained from the wave-vector change rate  $dk_x/dt$  using the fact that any nonzero change of the parameters of the Hamiltonian leads to a finite nonadiabaticity described by  $\eta$  and given by the quantum metric along the wave-vector evolution direction [32]:

$$f_{NA} = \frac{g_{k_x, k_x}}{\hbar^2 \Omega^2} \left( \frac{dk_x}{dt} \right)^2 \quad (\text{B5})$$

This nonadiabatic fraction is linked with the angle between the spin and the effective field  $\eta$  as  $f_{NA} = \eta^2/4$ . This allows us to transform the expression obtained using the QM to the familiar expression with the Berry curvature:

$$\hbar v_y = \dots + 2\sqrt{g_{yy}g_{xx}} \frac{dk_x}{dt} = B_z \frac{dk_x}{dt}, \quad (\text{B6})$$

where we have used the identity

$$\sqrt{\det g} = \frac{B_z}{2} \quad (\text{B7})$$

valid for all two-band Hamiltonians with a Berry curvature of a constant sign [28]. The two approaches indeed give the same contribution to the transverse velocity.

### APPENDIX C: COMPARISON WITH CULCER'S EQUATIONS

The semiclassical equations of motion for a wave packet with the center-of-mass position  $\mathbf{r}_c$  and wave vector  $\mathbf{q}_c$ , were written in Ref. [15]:

$$\hbar \dot{\mathbf{q}}_c = -\frac{\partial E}{\partial \mathbf{r}_c} - \mathbf{B}_{tr}, \quad (\text{C1})$$

$$\hbar \dot{\mathbf{r}}_c = \frac{\partial E}{\partial \mathbf{k}_c} - \mathbf{B}_{qq} \dot{\mathbf{q}}_c + \mathbf{B}_{tq}, \quad (\text{C2})$$

$$i\hbar \frac{dc_i}{dt} = \left( H_{ij} - \hbar \left\langle u_i \left| i \frac{du_j}{dt} \right. \right\rangle \right) c_j \quad (\text{C3})$$

with the coefficients  $c_i$  determining the composition of the wave packet within the bands with the numbers  $i$ ,  $u_i$  being the periodic spinor part of the wave packet wave function,  $\mathbf{B}_{qq}$  is the Berry curvature tensor, calculated not for a single band, but for a superposition of bands, and

$$B_{tq}^\alpha = i \left( \left\langle \frac{\partial u}{\partial t} \left| \frac{\partial u}{\partial q_\alpha} \right. \right\rangle - \left\langle \frac{\partial u}{\partial q_\alpha} \left| \frac{\partial u}{\partial t} \right. \right\rangle \right) \quad (\text{C4})$$

is an additional Berry curvature tensor  $\mathbf{B}_{tq}$  which appears because of the explicit time dependence  $u(t)$  (absent in the case of a single band).

### APPENDIX D: QUANTUM METRIC AND THE NON-ABELIAN GAUGE FIELD

A general nonrelativistic Hamiltonian of a massive matter field (quantum particle) minimally coupled with a non-Abelian gauge field determined by a vector potential  $A_\mu^a$  reads [37,40,41]:

$$H_{YM} = \frac{1}{2m} (\hat{\mathbf{p}} - \eta \mathbf{A}^a \sigma^a)^2 + \eta A_t^a \sigma^a. \quad (\text{D1})$$

The coupling constant is  $\eta = \hbar/2$  (the quantum of spin). We use upper number indices 0 – 3 for Pauli matrices. Comparing this expression with the Rashba Hamiltonian [Eq. (8) of the main text], one sees that only two components of the vector potential are nonzero:  $A_x^1 = -m\alpha/\eta$ ,  $A_y^2 = -m\alpha/\eta$ . The non-Abelian nature of the field makes that the constant vector potential nevertheless gives rise to nonzero field strength tensor. In the case of Rashba SOC, the only nonzero components are  $F_{yx}^3 = -F_{xy}^3 = -m^2\alpha^2/\eta$ . This nonzero field is responsible for an analog of a Lorentz force for a non-Abelian gauge field.

The Yang-Mills theory thus allows us to predict an analog of a transverse force acting on a spin current in the Rashba Hamiltonian. This force is proportional to the field strength and to the spin current, as can be seen from the second Newton's law:

$$m dv^\mu/d\tau = \mathbf{J}_v \cdot \mathbf{F}^{\mu\nu}. \quad (\text{D2})$$

The corresponding acceleration is ultimately found as  $a_x = -2m\alpha^2 J_y^3/\hbar^2$ ,  $a_y = 2m\alpha^2 J_x^3/\hbar^2$ , where  $J_x^3$ ,  $J_y^3$  are the circular (spin-up/down) components of the spin current propagating along  $x$  and  $y$ , respectively.

We will now compare the predictions of the Yang-Mills theory with those of the semiclassical equations that we have derived. In the particular case where the external forces are absent, the first of the equations of motion (5) of the main text gives that the central wave vector of the wave packet is constant:  $\dot{\mathbf{k}} = 0$ . The equation (6) of the main text is still time dependent, so it can be derived once again to find an analog of the second Newton's law, similar to Eq. (D2). We consider a parabolic band extremum characterized by an effective mass  $m$ , and define the  $z$  projection of the spin current as  $\mathbf{J} = \hbar^2 \mathbf{q}_c \cos \theta_s/2m$ , which allows writing

$$m \ddot{\mathbf{r}} = \sqrt{g_{kk}} \frac{4\alpha^2 km}{\hbar^2} \mathbf{e}_z \times \mathbf{J} \quad (\text{D3})$$

making the metric appear explicitly in the expression for the non-Abelian magneticlike Yang-Mills force. We can therefore conclude that the QM is at the heart of the microscopic mechanism behind the Lorentz-like transverse force acting on a spin current in the static non-Abelian gauge field described by Eq. (D2).

The covariant derivative appears in the Lagrangian to ensure the fundamental principle of gauge invariance. But the physical mechanism associated with its microscopic effect is based on the fact that the group velocity in a spinor system necessarily includes the QM describing the interband transitions due to the spin dynamics.

### APPENDIX E: ESTIMATION OF THE MAXIMAL VALUES OF THE EFFECTS

We note that the scale of both the AHE and the ZBW is quite comparable in both configurations (TE-TM or Rashba SOCs + Zeeman splitting), in what concerns the maximal lateral deviation, maximal velocity, or maximal acceleration. In general, the ZBW is larger above a certain wave vector. We note that the combination of the Rashba SOC with the Zeeman splitting is equivalent (in what concerns its spinor part) to the gapped Dirac Hamiltonian. This makes the applicability of our example even broader.

The pure AHE determined by the Berry curvature requires adiabatic evolution of the system. The additional group velocity due to AHE is given by  $\dot{\mathbf{q}}_{\text{AHE}} = \mathbf{B} \times \dot{\mathbf{k}}$ , and if the potential gradient is constant, the acceleration due to AHE can be found as  $\ddot{\mathbf{q}}_{\text{AHE}} = \dot{\mathbf{B}} \times \dot{\mathbf{k}}$ . We consider a wave packet accelerated from  $k = 0$  along the  $x$  axis. The transverse acceleration therefore can be found as

$$\frac{d^2 r_y}{dt^2} = \frac{dB_z}{dk_x} \left( \frac{dk_x}{dt} \right)^2. \quad (\text{E1})$$

To find the maximal acceleration we need to find the maximal value of  $dB_z/dk_x$ , which occurs at  $k_{\max} \approx 0.48\sqrt{\Delta/\beta}$ , which gives

$$\left(\frac{dB_z}{dk_x}\right)_{\max} \approx 1.51 \frac{\beta^{3/2}}{\Delta^{3/2}}. \quad (\text{E2})$$

On the other hand, the maximal value of the acceleration  $dk_x/dt$  acceptable for the adiabatic evolution can be obtained from the expression for the nonadiabatic fraction [32]:

$$f_{\text{NA}} = \frac{g_{kk}}{\Omega^2} \left(\frac{dk_x}{dt}\right)^2. \quad (\text{E3})$$

Requiring that the nonadiabatic fraction does not exceed 20% gives the maximal value of the square of the derivative

$$\left(\frac{dk_x}{dt}\right)_{\max}^2 \approx \frac{\Delta^3}{\hbar^2 \beta}. \quad (\text{E4})$$

Qualitatively, the same condition can be obtained from the physical requirement that the energy of the eigenstate should not change faster than the value of the frequency corresponding to the splitting between the eigenstates.

Putting both expressions together, we find  $a_{\text{AHE},\max} \approx 1.5\beta^{1/2}\Delta^{3/2}/\hbar^2$ . On the other hand, the maximal acceleration due to the QM depends on the wave vector, which for the system with TE-TM SOC (and without the Zeeman splitting) gives  $a_{\text{ZBW},\max} = \Omega^2 \sqrt{g_{yy}} = 4\beta^2 k^3/\hbar^2$ . Comparing both expressions, we see that for  $k > 2^{-2/3}\sqrt{\Delta/\beta}$ , the ZBW acceleration is larger than the AHE one, whereas for the wave vector where the AHE acceleration is maximal, it is approx-

imately twice larger than the ZBW:  $a_{\text{AHE},\max} \approx 2a_{\text{ZBW}}(k_{\max})$ . The ZBW acceleration can be increased unlimitedly by increasing the wave vector  $k_x$ .

For the configuration with Rashba SOC and Zeeman splitting, the accelerations are given by  $a_{\text{AHE},\max} \approx 0.43\alpha\Delta/\hbar^2$  and  $a_{\text{ZBW},\max} = 2\alpha^2 k/\hbar^2$ . For the same wave vector  $k_{\max} = \Delta/2\alpha$  (giving the maximal AHE acceleration), one finds  $a_{\text{AHE},\max} \approx 0.43a_{\text{ZBW},k_{\max}}$ . The AHE acceleration is therefore smaller than the ZBW one at this wave vector. However, for this configuration, it is better to compare the transverse velocities, and not the accelerations, because the AHE acceleration is actually reducing the effect (there is a nonzero transverse velocity at  $t = 0$ , which then decays).

The expressions for the maximal velocities give the same result  $v_{\text{AHE},\max} = v_{\text{ZBW},\max} = \alpha/2\hbar$ . It is also interesting to compare the maximal lateral shift in both cases. Both AHE and ZBW shifts exhibit a divergent behavior on a certain parameter ( $\Delta_Z$  for AHE,  $k_0$  for ZBW), and can, in principle, exhibit arbitrarily large values, if these two parameters are decreased. On the other hand, the experimental observations are limited by the line broadening  $\Gamma$  (due to finite lifetime) and by the wave packet size in real space. For the Rashba Hamiltonian, the broadening sets a common limit for both effects:  $\Delta Y_{\text{AHE/ZBW},\max} \sim \alpha/\Gamma$ . The wave packet size also sets a similar limit:  $\Delta Y_{\text{AHE/ZBW},\max} \sim 1/\sigma_k \sim \sigma_r$ ; the maximal scale of both effects is determined by the wave packet size. For AHE, this condition means the WP should be smaller than the region with nonzero Berry curvature, and for ZBW that  $k_0$  is really different from 0. We conclude that while the two effects occur in completely different regimes (adiabatic vs coherent oscillations), their scales are actually quite comparable.

- 
- [1] H. Jones and C. Zener, *Proc. R. Soc. London Ser. A* **144**, 101 (1934).
- [2] J. Zak, *Phys. Rev.* **168**, 686 (1968).
- [3] G. Sundaram and Q. Niu, *Phys. Rev. B* **59**, 14915 (1999).
- [4] R. Karplus and J. M. Luttinger, *Phys. Rev.* **95**, 1154 (1954).
- [5] J. Provost and G. Vallee, *Commun. Math. Phys.* **76**, 289 (1980).
- [6] M. V. Berry, *Proc. R. Soc. London, Ser. A* **392**, 45 (1984).
- [7] M. Berry, in *Geometric Phases in Physics* (World Scientific, Singapore, 1989), p. 7.
- [8] K. v. Klitzing, G. Dorda, and M. Pepper, *Phys. Rev. Lett.* **45**, 494 (1980).
- [9] D. J. Thouless, M. Kohmoto, M. P. Nightingale, and M. den Nijs, *Phys. Rev. Lett.* **49**, 405 (1982).
- [10] M. Z. Hasan and C. L. Kane, *Rev. Mod. Phys.* **82**, 3045 (2010).
- [11] L. Lu, J. D. Joannopoulos, and M. Soljačić, *Nat. Photon.* **8**, 821 (2014).
- [12] G. Ma, M. Xiao, and C. T. Chan, *Nat. Rev. Phys.* **1**, 281 (2019).
- [13] D. D. Solnyshkov, G. Malpuech, P. St-Jean, S. Ravets, J. Bloch, and A. Amo, *Opt. Mater. Express* **11**, 1119 (2021).
- [14] M.-C. Chang and Q. Niu, *J. Phys.: Condens. Matter* **20**, 193202 (2008).
- [15] D. Culcer, Y. Yao, and Q. Niu, *Phys. Rev. B* **72**, 085110 (2005).
- [16] M. Di Liberto, N. Goldman, and G. Palumbo, *Nat. Commun.* **11**, 5942 (2020).
- [17] P. Zanardi, P. Giorda, and M. Cozzini, *Phys. Rev. Lett.* **99**, 100603 (2007).
- [18] Y. Gao, S. A. Yang, and Q. Niu, *Phys. Rev. Lett.* **112**, 166601 (2014).
- [19] F. Piéchon, A. Raoux, J.-N. Fuchs, and G. Montambaux, *Phys. Rev. B* **94**, 134423 (2016).
- [20] A. Srivastava and A. Imamoglu, *Phys. Rev. Lett.* **115**, 166802 (2015).
- [21] S. Peotta and P. Törmä, *Nat. Commun.* **6**, 8944 (2015).
- [22] L. Liang, S. Peotta, A. Harju, and P. Törmä, *Phys. Rev. B* **96**, 064511 (2017).
- [23] M. Kremer, L. Teuber, A. Szameit, and S. Scheel, *Phys. Rev. Res.* **1**, 033117 (2019).
- [24] G. Salerno, N. Goldman, and G. Palumbo, *Phys. Rev. Res.* **2**, 013224 (2020).
- [25] Yu-Quan Ma, Shi-Jian Gu, Shu Chen, Heng Fan, and Wu-Ming Liu, *Europhys. Lett.* **103**, 10008 (2013).
- [26] R. Roy, *Phys. Rev. B* **90**, 165139 (2014).
- [27] T. S. Jackson, G. Möller, and R. Roy, *Nat. Commun.* **6**, 8629 (2015).
- [28] B. Mera and T. Ozawa, *Phys. Rev. B* **104**, 045104 (2021).
- [29] X. Tan, D. W. Zhang, Z. Yang, J. Chu, Y. Q. Zhu, D. Li, X. Yang, S. Song, Z. Han, Z. Li, Y. Dong, H. F. Yu, H. Yan, S. L. Zhu, and Y. Yu, *Phys. Rev. Lett.* **122**, 210401 (2019).

- [30] M. Yu, P. Yang, M. Gong, Q. Cao, Q. Lu, H. Liu, S. Zhang, M. B. Plenio, F. Jelezko, T. Ozawa *et al.*, *Nat. Sci. Rev.* **7**, 254 (2019).
- [31] A. Gianfrate, O. Bleu, L. Dominici, V. Ardizzone, M. De Giorgi, D. Ballarini, G. Lerario, K. West, L. Pfeiffer, D. Solnyshkov *et al.*, *Nature (London)* **578**, 381 (2020).
- [32] O. Bleu, G. Malpuech, Y. Gao, and D. D. Solnyshkov, *Phys. Rev. Lett.* **121**, 020401 (2018).
- [33] T. Holder, D. Kaplan, and B. Yan, *Phys. Rev. Research* **2**, 033100 (2020).
- [34] Y. Gao and D. Xiao, *Phys. Rev. Lett.* **122**, 227402 (2019).
- [35] D. D. Solnyshkov, C. Leblanc, L. Bessonart, A. Nalitov, J. Ren, Q. Liao, F. Li, and G. Malpuech, *Phys. Rev. B* **103**, 125302 (2021).
- [36] S.-Q. Shen, *Phys. Rev. Lett.* **95**, 187203 (2005).
- [37] P.-Q. Jin, Y.-Q. Li, and F.-C. Zhang, *J. Phys. A* **39**, 7115 (2006).
- [38] N. Hatano, R. Shirasaki, and H. Nakamura, *Phys. Rev. A* **75**, 032107 (2007).
- [39] J.-S. Yang, X.-G. He, S.-H. Chen, and C.-R. Chang, *Phys. Rev. B* **78**, 085312 (2008).
- [40] C. N. Yang and R. L. Mills, *Phys. Rev.* **96**, 191 (1954).
- [41] L. H. Ryder, *Quantum Field Theory: Second Edition* (Cambridge University Press, Cambridge, 1996).
- [42] H. Tercas, H. Flayac, D. D. Solnyshkov, and G. Malpuech, *Phys. Rev. Lett.* **112**, 066402 (2014).
- [43] Y. Chen, R.-Y. Zhang, Z. Xiong, Z. Hong Hang, J. Li, J. Q. Shen, and C. T. Chan, *Nat. Commun.* **10**, 3125 (2019).
- [44] Y. Yang, C. Peng, D. Zhu, H. Buljan, J. D. Joannopoulos, B. Zhen, and M. Soljacic, *Science* **365**, 1021 (2019).
- [45] A. Fieramosca, L. Polimeno, G. Lerario, L. De Marco, M. De Giorgi, D. Ballarini, L. Dominici, V. Ardizzone, M. Pugliese, V. Maiorano *et al.*, [arXiv:1912.09684](https://arxiv.org/abs/1912.09684).
- [46] R. Winkler, U. Zülicke, and J. Bolte, *Phys. Rev. B* **75**, 205314 (2007).
- [47] W. Zawadzki and T. M. Rusin, *J. Phys.: Condens. Matter* **23**, 143201 (2011).
- [48] S. A. Tarasenko, A. V. Poshakinskiy, E. L. Ivchenko, I. Stepanov, M. Ersfeld, M. Lepsa, and B. Beschoten, *JETP Lett.* **108**, 326 (2018).
- [49] R. Gerritsma, G. Kirchmair, F. Zähringer, E. Solano, R. Blatt, and C. Roos, *Nature (London)* **463**, 68 (2010).
- [50] L. J. LeBlanc, M. C. Beeler, K. Jiménez-García, A. R. Perry, S. Sugawa, R. A. Williams, and I. B. Spielman, *New J. Phys.* **15**, 073011 (2013).
- [51] C. Qu, C. Hamner, M. Gong, C. Zhang, and P. Engels, *Phys. Rev. A* **88**, 021604(R) (2013).
- [52] F. Dreisow, M. Heinrich, R. Keil, A. Tünnermann, S. Nolte, S. Longhi, and A. Szameit, *Phys. Rev. Lett.* **105**, 143902 (2010).
- [53] Q. Guo, W. Gao, J. Chen, Y. Liu, and S. Zhang, *Phys. Rev. Lett.* **115**, 067402 (2015).
- [54] R.-P. Guo, Q.-H. Guo, L.-T. Wu, J. Chen, and D. Fan, *Opt. Express* **24**, 13788 (2016).
- [55] T. L. Silva, E. R. F. Tallebois, R. M. Gomes, S. P. Walborn, and A. T. Avelar, *Phys. Rev. A* **99**, 022332 (2019).
- [56] E. S. Sedov, Y. G. Rubo, and A. V. Kavokin, *Phys. Rev. B* **97**, 245312 (2018).
- [57] E. S. Sedov, I. E. Sedova, S. M. Arakelian, and A. V. Kavokin, *New J. Phys.* **22**, 083059 (2020).
- [58] M. Iskin, *Phys. Rev. A* **99**, 053603 (2019).
- [59] R. P. Feynman, F. L. Vernon Jr., and R. W. Hellwarth, *J. Appl. Phys.* **28**, 49 (1957).
- [60] L. Casetti, M. Pettini, and E. Cohen, *Phys. Rep.* **337**, 237 (2000).
- [61] P. Rashevsky, *Riemannian Geometry and Tensor Analysis* (Nauka, Moscow, 1967).
- [62] J. A. Lock, *Am. J. Phys.* **47**, 797 (1979).
- [63] D. Xiao, Y. Yao, Z. Fang, and Q. Niu, *Phys. Rev. Lett.* **97**, 026603 (2006).
- [64] A. Kavokin, G. Malpuech, and M. Glazov, *Phys. Rev. Lett.* **95**, 136601 (2005).
- [65] L. Liang, T. I. Vanhala, S. Peotta, T. Siro, A. Harju, and P. Törmä, *Phys. Rev. B* **95**, 024515 (2017).